AIAA Journal

VOLUME 8 JUNE 1970 NUMBER 6

Influence of a Supersonic Flowfield on the Elastic Stability of Cylindrical Shells

GERALD W. BARR*
Sandia Laboratories, Albuquerque, N. Mex.

AND

RONALD O. STEARMAN†
University of Texas, Austin, Texas

The rather complex interaction problem of shell divergence and panel flutter that may be encountered by an aerospace vehicle during the boost phase of a trajectory is treated theoretically and the results then compared qualitatively with recent experimental observations. The analytical model considers the combined influence of internal pressure and axial compressive loading on a thin-walled cylindrical shell in a supersonic flowfield. Radial edge constraint and initial imperfections also are considered. The formulation employs the nonlinear Donnell shell equations and a linear "piston theory" aerodynamic approximation and utilizes a kinetic stability approach. The aeroelastic stability of the shell is determined about its deformed middle surface using Galerkin's technique in a modal solution. The results of the analysis indicate that the supersonic flowfield has no effect on the critical buckling load or the unstable mode of the shell. Small amounts of axial loading, however, were found to reduce significantly the critical panel flutter speed of the shell. These results were verified, at least qualitatively, in recent wind-tunnel tests on shell models.

Nomenclature

A = equivalent linear matrix, 2N × 2N
B_0,B_1,B_2,B_3 = matrices, dynamic stability problem
D = flexural rigidity, $Eh^3/12(1-\nu^2)$
E = Young's modulus of elasticity
F = stress function
$\tilde{F}$ = F/Eh^3
$f(\alpha)$ = axial dependence of displacement
$g(\alpha)$ = axial dependence of stress function
h = thickness of shell
I = identity matrix, $2N \times 2N$
k = reduced frequency, $\omega R/U = \bar{k} + ik^*$ / = eigenvalue of nonlinear stability problem
L = cylinder length
m = axial half waves of unstable mode
M = Mach number
N = number of assumed modes
n = circumferential wave number
N_x,N_y,N_{xy} = midplane stress resultants
$\bar{N}_x$ = applied axial stress resultant
$\tilde{N}_x$ = buckling load ratio, $\bar{N}_xR[3(1-\nu^2)]^{1/2}/Eh^2$
p = net radial outward surface pressure
p_a = radial aerodynamic component
$\bar{p}$ = pressure differential across shell skin, positive for tensile hoop stress, psig
$\tilde{p}$ = $\bar{P}/E(R/h)^2[12(1-\nu^2)^{1/2}/\pi^2]$
p_∞ = freestream static pressure
q = dynamic pressure, $\frac{1}{2}\rho_\infty U^2 = (\gamma/2)\,p_\infty M^2$
R = cylinder radius
t = time
u,v,w = middle surface displacements: axial, circumferential, and radial, respectively
U = freestream velocity
$\bar{w}_r$ = initial imperfection, $\bar{\mu}\sin(r\pi x/L)$
$\tilde{w}_r$ = $\bar{w}_r/h$
x,y,z = coordinate axes, see Fig. 1
X_m,Y_m = coefficients of displacements and stress functions series
Z_m = $m\pi/(L/R)$
α = x/R
β = Mach number parameter $(M^2-1)^{1/2}$
γ = adiabatic exponent
γ_{xy} = shearing strain component
δ_k = roots of homogeneous part of static problem
ϵ_x,ϵ_y = normal strain components
Θ = y/R
$\bar{\mu}$ = imperfection amplitude
ν = Poisson's ratio
ρ_s = shell density
ρ_∞ = freestream density
τ = time, Ut/R
$(\ )_s$ = static component of $(\ )$

Received April 4, 1969; revision received October 13, 1969. Work performed under the auspices of the Air Force Office of Scientific Research, Arnold Engineering Development Center, and the Atomic Energy Commission.

* Staff Member, Dynamic Analysis Research Division. Member AIAA.

† Associate Professor, Department of Aerospace and Engineering Mechanics. Member AIAA.

$( )_0$ = dynamic component of ( )
$\tilde{( )}$ = nondimensional form of ( )
$\tilde{\nabla}^4$ = $[( ),_{\alpha\alpha\alpha\alpha} + 2( ),_{\alpha\alpha\theta\theta} + ( ),_{\theta\theta\theta\theta}]$

1. Introduction

THE structural loads imposed on many aerospace vehicles passing through the region of maximum dynamic pressure during the boost phase of a trajectory are quite severe and may result in the structure becoming aeroelastically unstable in either a static or a dynamic mode, i.e., diverging or fluttering, respectively. Since the primary structural member is usually the thin-walled cylindrical shell, the stability of this type of structure is of fundamental concern to the designer. The primary objective of this investigation is to obtain the combination of applied stress states in the shell for which the critical mode of the aeroelastic instability will be shell divergence rather than shell flutter. The applied stress state is due to internal pressure, axial load, and external flow conditions. The influence of 1) the supersonic flowfield on the critical buckling load of the shell, and 2) the axial compressive loading on the dynamic aeroelastic flutter boundary will be determined.

Stearman[1] in 1962 and Olson[2] in 1964 conducted supersonic wind-tunnel studies on the aeroelastic stability of thin-walled cylindrical shells. During these studies, shell buckling under external hydrostatic pressure and under a combined internal pressure and axial compressive load were investigated in the presence of an external supersonic flowfield parallel to the shell's axis. The results of the buckling studies did indicate that the supersonic flowfield had a slightly destabilizing or negligible influence on the critical buckling load. Only a limited amount of experimental data were obtained during these wind-tunnel tests because of the difficulty and expense involved in performing this type of investigation. Therefore, to gain better insight into the basic features of the problem before extensive wind-tunnel experiments were performed, the authors felt that this rather complex problem should be investigated from an analytical point of view initially, attempting only qualitative comparisons with the limited amount of experimental data available to date.

2. Theoretical Analysis

The theoretical portion of the study investigates the aeroelastic stability characteristics of thin-walled finite length cylindrical shells having large radius to thickness ratios and small initial deviations of the median surface from that of a perfect cylindrical shell. The analytical model under study, flow condition, coordinate systems, and static loading conditions are shown in Fig. 1. The initial imperfections are axisymmetric having a harmonic wave form in the axial direction. The outer surface of the shell is exposed to a supersonic flow parallel to the shell's axis. Static loading consists of a combined internal pressure and/or axial compressive loading.

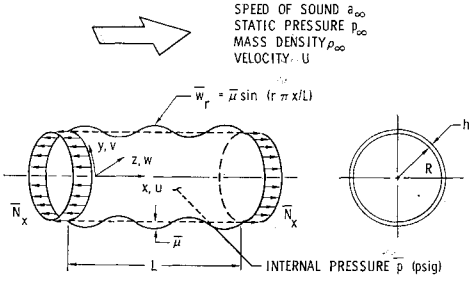

Fig. 1 Shell geometry and flow conditions.

2.1 Problem Formulation

The present analysis investigates the aeroelastic stability of the shell about its deformed middle surface utilizing a kinetic stability approach. The initial geometric imperfections and the prestability deformations, resulting from the interaction of the initial imperfections and radial edge constraint with the static preload, constitute the deformed middle surface of the shell. A set of nonlinear Donnell type shell equations coupled with a linear piston theory aerodynamic approximation are used to describe the motion of the shell and the radial surface loading due to the supersonic flowfield. The geometric nonlinearities along with the initial imperfections are introduced into the shell theory through the strain-displacement relations. In-plane inertia has been neglected in the equation of motion due to the predominantly radial motion of the shell. The governing equations of motion of a cylindrical shell with initial deviations of the median surface are written in terms of the radial displacement w, and the total stress function F, as

$$\frac{1}{Eh}\nabla^4 F = w^2_{,xy} - w_{,xx}w_{,yy} + \frac{1}{R}w_{,xx} - \bar{w}_{r,xx}w_{,yy} - \bar{w}_{r,yy}w_{,xx} + 2\bar{w}_{r,xy}w_{,xy} \quad (1)$$

$$D\nabla^4 w + \frac{1}{R}F_{,xx} - F_{,yy}(w_{,xx} + \bar{w}_{r,xx}) - F_{,xx}(w_{,yy} + \bar{w}_{r,yy}) + 2F_{,xy}(w_{,xy} + \bar{w}_{r,xy}) = p(x,y,t) \quad (2)$$

where the commas denote partial differentiation. The first expression is a compatibility relationship and the second is the displacement equilibrium relation. The associated boundary conditions of a shell with simply supported "zero tangential shear stress" edges at $x = 0,L$ are

$$w(x,y,t) = w(x,y,t)_{,xx} = F(x,y,t)_{,xy} = 0$$
$$F(x,y,t)_{,yy} = \bar{N}_x \quad (3)$$

which represent vanishing radial displacement, moment, and tangential shear stress with the axial stress equal to the applied axial stress. These conditions were felt to more nearly represent the boundary conditions imposed by the wind-tunnel test model on the experimental shells that are used to substantiate the theoretical results, at least qualitatively. The influence of different structural boundary conditions are discussed in the literature.[3,4]

The surface loading may be defined as

$$p(x,y,t) = \bar{p} - \rho_s h\ddot{w} + p_a \quad (4)$$

where the first term is the pressure differential across the skin of the shell and the second term is the inertial loading resulting from the motion of the surface. The radial aerodynamic pressure is approximated by a first-order piston theory, with a curvature correction term, to the more exact linearized

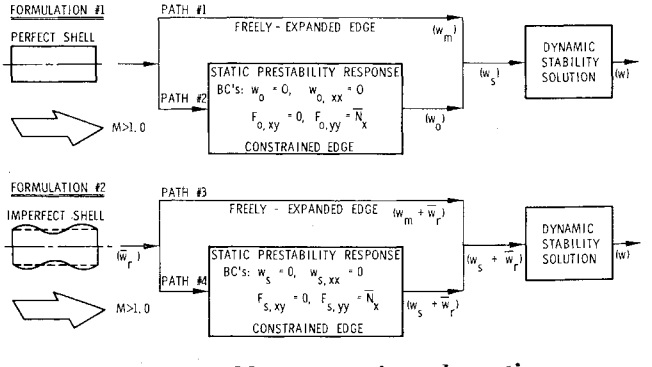

Fig. 2 Problem separation schematic.

potential flow expression as

$$p_a = -\frac{2q}{\beta}\left\{\hat{w}_{,x} + \frac{1}{U}\left(\frac{\beta^2-1}{\beta^2}\right)\hat{w}_{,t} - \frac{1}{2\beta R}\hat{w}\right\} \quad (5)$$

where $\hat{w}$ is the total displacement of the middle surface with respect to a perfect cylinder.

Recent experimental observations[5] cast serious doubt as to the validity of employing linear piston theory to describe the unsteady pressure field over the shell because of the strong influence of the viscous boundary layer. Earlier experimental[6] studies however, do indicate that the static component of the aerodynamic pressure field can be represented adequately by such simple approximations. Consequently, this aerodynamic approximation should be adequate for the static aeroelastic stability problems of interest in the present study.

The analysis has been separated into two major formulations that are illustrated schematically in Fig. 2. The first formulation[3] considers a perfect cylindrical shell, whereas the second formulation[4] considers the shell to have axisymmetric initial imperfections of harmonic waveform. Both formulations contain the so-called classical analysis, PATHS #1 and #3, and a nonclassical analysis, PATH #2 and #4, as special cases. The classical analysis considers only a kinetic stability solution with respect to the undeformed middle surface of a freely expanded membrane shell. The nonclassical approach, on the other hand, determines the statically deformed middle surface due to the initial loading conditions and then determines the stability of the shell about the deformed middle surface with the kinetic stability approach. A fairly detailed account of these analyses can be found in Ref. 4 and therefore, only a brief description will be presented in this paper.

A complete consistent solution to the stability problem is accomplished in two steps. The first step determines the prestability deformation of the middle surface due to the application of initial preloads and radial pressure from the airstream. This deformation is obtained in closed form from a set of steady-state response equations obtained by separating Eqs. (1) and (2) into their static and dynamic components by making the following substitutions:

$$\begin{aligned} w(x,y,t) &= w_s(x) + w^0(x,y,t) \\ F(x,y,t) &= F_s(x,y) + F^0(x,y,t) \\ p(x,y,t) &= p_s(x) + p^0(x,y,t) \end{aligned} \quad (6)$$

This is possible because of the axisymmetric property of the initial imperfections, the surface loading, and the resulting prestability deformations. A set of equations governing the static prestability deformations (subscript s) is obtained by virtue of preflutter equilibrium. A second set of equations in terms of the dynamic components (superscript 0) govern the dynamic stability of the shell about its deformed middle surface. The two systems of equations are coupled through the induced static deformation and stress terms.

2.2 Static Prestability Response

The deformed middle surface of the shell is determined from the set of steady-state response equations

$$Dw_{s,xxxx} + (1/R)F_{s,xx} - F_{s,yy}w_{s,xx} = p_s(x) + F_{s,yy}\bar{w}_{r,xx} \quad (7)$$

and

$$(1/Eh)\nabla^4 F_s = (1/R)w_{s,xx} \quad (8)$$

where the static component of the radial surface loading is

$$p_s(x) = \bar{p} - (2q/\beta)\{(w_s + \bar{w}_r)_{,x} - (1/2\beta R)(w_s + \bar{w}_r)\} \quad (9)$$

The associated boundary conditions at $x = 0,L$ are

$$w_s(x) = w_s(x)_{,xx} = F_s(x,y)_{,xy} = 0;\ F_s(x,y)_{,yy} = \bar{N}_x \quad (10)$$

The general analytical solution consists of reducing Eqs. (7) and (8) to a single equivalent equation of motion

$$Dw_s^{IV} - \bar{N}_x w_s^{II} + (Eh/R^2)w_s = p_s(x) - (\nu/R)\bar{N}_x + \bar{N}_x\bar{w}_r^{II} \quad (11)$$

with the initial geometric imperfection defined by

$$\bar{w}_r = \bar{\mu}\sin(r\pi x/L) \quad (12)$$

where $\bar{\mu}$ is the prescribed amplitude of the imperfection. The resulting nondimensional deformation shapes have the form

$$\bar{w}_s(\alpha) = \sum_{k=1}^{4} C_k e^{\delta_k \alpha} + K_1 + K_2\cos Z_r\alpha + K_3\sin Z_r\alpha \quad (13)$$

where the δ'_ks are the roots of the characteristic polynomial of the homogeneous solution and the C'_ks are obtained by applying the boundary conditions. The constant K_1 is associated with the freely expanded radial deformation of an unconstrained shell and K_2 and K_3 are constants associated with the initial imperfection shape.

2.3 Dynamic Stability Solutions

In the second step, the dynamic stability of the shell was investigated by perturbing the shell's middle surface with an oscillatory motion of infinitesimal amplitude. Therefore, the set of governing equations will be nonlinear partial differential equations with variable coefficients. Linearization is accomplished by neglecting products of the dynamic components. These linearized dynamic stability equations have the form

$$D\nabla^4 w^0 + \frac{1}{R}F^0_{,xx} - F_{s,yy}w^0_{,xx} - F_{s,xx}w^0_{,yy} - F^0_{,yy}(w''_s + \bar{w}''_r) + 2F_{s,xy}w^0_{,xy} = p^0(x,y,t) \quad (14)$$

and

$$\frac{1}{Eh}\nabla^4 F^0 = \frac{1}{R}w^0_{,xx} - (w''_s + \bar{w}''_r)w^0_{,yy} \quad (15)$$

where the dynamic component of the surface loading is

$$p^0(x,y,t) = -\rho_s h w^0_{,tt} - \frac{2q}{\beta}\left\{w^0_{,x} + \frac{1}{U}\left(\frac{\beta^2-1}{\beta^2}\right)w^0_{,t} - \frac{1}{2\beta R}w^0\right\} \quad (16)$$

The primes denote ordinary differentiation with respect to x. The associated boundary conditions at $x = 0,L$ are

$$w^0(x,y,t) = w^0(x,y,t)_{,xx} = F^0(x,y,t)_{,xy} = F^0(x,y,t)_{,yy} = 0 \quad (17)$$

Modal solutions of the following form are assumed:

$$\begin{aligned} \tilde{w}^0(\alpha,\theta,\tau) &= f(\alpha)\cos n\theta e^{ik\tau} \\ \tilde{F}^0(\alpha,\theta,\tau) &= g(\alpha)\cos n\theta e^{ik\tau} \end{aligned} \quad (18)$$

where the axial deformation function and the axial stress function satisfying the boundary conditions are denoted by

$$\begin{aligned} f(\alpha) &= \sum_{m=1}^{N} \tilde{X}_m \sin Z_m\alpha \\ g(\alpha) &= \sum_{m=1}^{N} \tilde{Y}_m \sin Z_1\alpha \sin Z_m\alpha \end{aligned} \quad (19)$$

Galerkin's approximation was applied simultaneously to Eqs. (14) and (15) to reduce the stability problem to a non-

linear eigenvalue problem of the form

$$[k^2B_0 - kB_1 - B_2]\tilde{\mathbf{X}} = 0 \tag{20}$$

The reduced frequency, $k = \omega R/U = \bar{k} + ik^*$, was considered to be the eigenvalue. An equivalent linear eigenvalue problem

$$\det[A - kI] = 0 \tag{21}$$

having the same eigenvalues as Eq. (20) was obtained with an equivalent matrix A defined by

$$A = \begin{bmatrix} B_0^{-1}B_1 & E \\ B_0^{-1}B_2 & O \end{bmatrix}_{2N \times 2N} \tag{22}$$

The identity matrix I is $2N \times 2N$, whereas the identity E is only $N \times N$. The procedure used to reduce this nonlinear problem, Eq. (20), to an equivalent linear relation has been developed by Franklin[7] and Guderley.[8]

2.4 Static Buckling Problem

The invacuo elastic stability or buckling of a thin cylindrical shell also is investigated using the kinetic stability approach. This stability approach poses the question "What is the value of the load for which the most general free motion of the system ceases to be bounded?" In reality, the kinetic method employs a standard vibration analysis in which the applied axial loading, $\tilde{N}_x$, is a free parameter. The critical buckling load is obtained by tracing the natural frequencies of the shell as the axial load increases. When the critical buckling load is approached, from the stable side, one of the modal frequencies of the shell will tend to zero. Therefore, the axial load that causes this frequency to vanish is considered to be the critical buckling load.

The vibration or kinetic buckling solution and the aeroelastic stability solution are very similar except that all the aerodynamic terms vanish, i.e., $B_1 = 0$, in the vibration problem. Therefore, the nonlinear eigenvalue problem, Eq. (20) reduces to

$$[k^2B_0 - B_2]\tilde{\mathbf{X}} = 0 \tag{23}$$

which may be recast in the form of a standard eigenvalue problem

$$[\bar{A} - \lambda I]\tilde{\mathbf{X}} = 0 \tag{24}$$

where $\bar{A} = B_0^{-1}B_2$ and $\lambda = k^2$. The eigenvalues can now be defined in terms of the natural frequencies of the shell, i.e., $k = \omega T$, which are nondimensionalized with respect to the period of oscillation T of the first axisymmetric vibration mode of an infinitely long cylindrical shell.

2.5 Stability Criteria

The stability criteria employed in this analysis is to observe the behavior of the eigenvalue, $k = \bar{k} + ik^*$, as a function of the freestream static pressure or applied axial load. The oscillatory motion of the shell is assumed to have the form

$$w^0(\alpha,\theta,\tau) \sim e^{ik\tau} = e^{i\bar{k}\tau}\, e^{-k^*\tau} \tag{25}$$

Considering this expression, the motion is seen to be oscillatory when $\bar{k} \neq 0$ and nonoscillatory when $\bar{k} = 0$. Also, the motion will be convergent (stable) if $k^* > 0$ and divergent (unstable) if $k^* < 0$. Therefore, the onset of the dynamic instability (flutter) may be defined as the point when k^* changes sign from positive to negative, i.e., $k^* = 0$, and the motion of the surface becomes undamped simple harmonic. Since aerodynamic buckling or divergence is a nonoscillatory type instability, the unstable eigenvalue is characterized by $\bar{k} = 0$ and $k^* < 0$. The kinetic buckling or vibration problem has been redefined such that the eigenvalue is denoted as $\lambda = k^2$. Therefore, the critical buckling load ratio is obtained by increasing $\tilde{N}_x$ until the $Re(\lambda) = (\bar{k}^2 - k^{*2})$ changes from positive to negative with a vanishing $Im(\lambda)$. This condition occurs when $\bar{k} = 0$ and $k^* = 0$.

2.6 Theoretical Results

The primary objective of the theoretical study is to determine the influence of an external supersonic flowfield on the critical buckling load of a finite length cylindrical shell. The axial compressive load, internal pressure, and freestream static pressure of the flowfield were varied to achieve different stress states. A shell geometry having a $L/R = 2.0$ and $R/h = 2000$ was chosen for this interaction study in order to obtain a qualitative correlation with existing experimental results. The shell is assumed to be initially perfect in an unstressed state with a Mach 3.0 supersonic flowfield parallel to the centerline of the shell. Both the buckling and aeroelastic stability boundaries were minimized with respect to the circumferential wave number, n.

The first step in this study was to characterize the elastic stability (buckling) behavior of the cylindrical shell with respect to a nondimensional shell internal pressure parameter $\tilde{p}$, and the axial load parameter, $\tilde{N}_x$. This study employed both the classical solution and the solution that includes the nonlinear prebuckling behavior of the shell. It was observed for the thin shell studied that the predeformations induced by the radial edge constraint did not affect the buckling phenomena. This is primarily because the edge constraint is felt only in a very narrow boundary-layer region near each edge of the shell. This buckling behavior is illustrated in Fig. 3 by comparing both solutions. An interesting trend to note in this figure is that even the classical solution exhibits a critical mode shape change of the buckling instability with increasing internal pressure. At zero internal pressure, the critical buckling mode shape is one of high-circumferential wave number, $n = 29$, which then degenerates to the axisymmetric instability shape as the in-

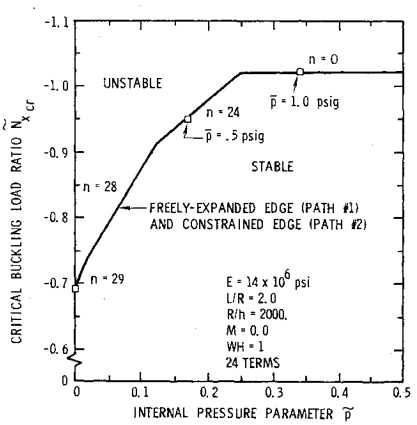

Fig. 3 Still air buckling interaction curve.

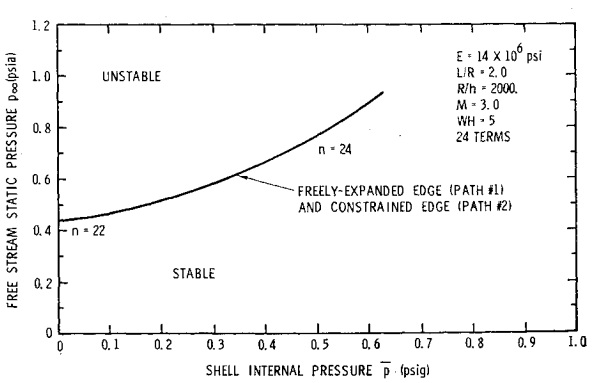

Fig. 4 Aeroelastic stability boundary at $\tilde{N}_x = 0$.

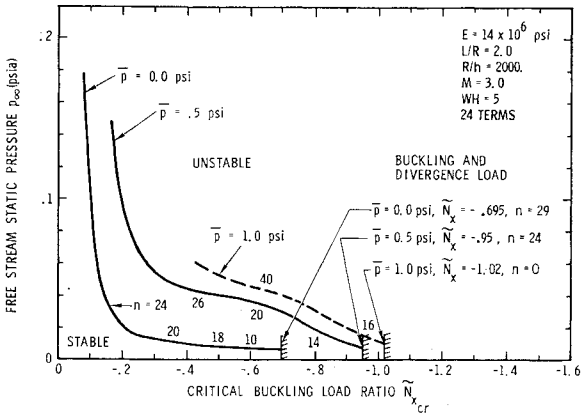

Fig. 5 Influence of axial compression loading on the aeroelastic stability boundary.

ternal pressure is increased. This trend has been observed experimentally for thin shells[9] but was not predicted theoretically by Almroth[10] for the thicker shell geometries and range of parameters studied.

The aeroelastic stability behavior for a shell with zero axial load is presented in Fig. 4 as a function of shell internal pressure. As in the buckling study, the influence of the nonlinear prebuckling behavior has a negligible effect on the stability boundary. Therefore, only the so-called classical formulation will be used to investigate the influence of the airstream on the critical buckling load of these thin shells.

The study to determine the critical stress states and flow conditions where divergence occurred instead of shell flutter was performed at discrete values of applied axial load and shell internal pressure. The freestream static pressure was then varied until an instability, flutter or divergence, occurred as defined by the stability criteria. Three different shell internal pressures were examined, $\bar{p} = 0.0, 0.5$, and 1.0 psig, and the corresponding stability boundaries are shown in Fig. 5. The complete aeroelastic stability boundary for the shell pressurized to 1.0 psig was not obtained because of the excessively large number of terms required to obtain complete convergence. The nonconverged stability boundary is represented by the dashed line. However, since the convergence character of the solution is different for the static and dynamic solutions, it is felt that the critical divergence load is predicted correctly. It can be seen that for each shell internal pressure level, the stability behavior exhibits a similar trend as a function of applied axial load. As the applied axial stress resultant $\bar{N}_x$, is increased, the ability of the shell to resist an aerodynamic flutter type instability decreases as much as 85–90% of the zero axial load case. This pronounced destabilizing trend occurs at axial loads less than 40% of the static still air buckling load of the shell.

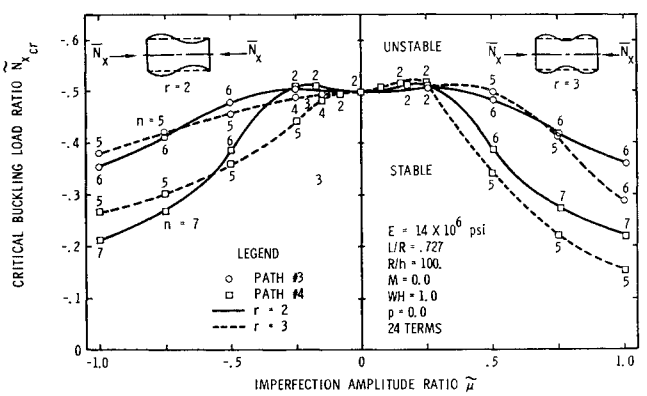

Fig. 6 Influence of the imperfection amplitude on the critical buckling load ratio.

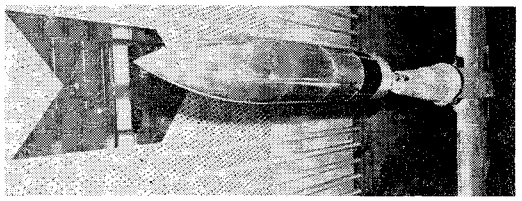

Fig. 7 Ogive-cylinder wind-tunnel flutter model.

The critical circumferential wave number is essentially constant in this range of axial load variation. For axial loads above approximately 40% of the critical buckling load, the freestream static pressure required to cause an aeroelastic instability remains fairly constant but the critical circumferential wave number decreases until a critical axial load is reached. At this axial load, the shell diverges into a static buckled shape with a corresponding circumferential wave number equivalent to that predicted from still air buckling studies. Also, the critical divergence axial load obtained in the presence of a supersonic flowfield is essentially the same as the critical buckling load predicted by the still air buckling study at corresponding shell internal pressures.

It is apparent from the aforementioned study that the axial load carrying capability of thin cylindrical shells is not influenced by the existence of an external supersonic flowfield. However, this does not preclude the necessity of investigating the dynamic stability of the shell since for certain flow and stress conditions the shell may be statically stable but dynamically unstable. This condition might exist in the region of maximum dynamic pressure during the boost phase of a trajectory where freestream static pressure is increasing rapidly and the applied axial load also is increasing due to aerodynamic drag and payload inertia.

The influence of axisymmetric initial geometric imperfections having a harmonic wave form in the axial direction on the still air buckling load was investigated using both solutions of formulation #2 in Fig. 2. A relatively thick (R/h = 100) short (L/R = 0.727) cylindrical shell having an asymmetric (r = 2) and a symmetric (r = 3) imperfection shape were investigated. The influence of the imperfection amplitude, ranging from zero for a perfect shell up to one shell thickness, on the critical buckling load is presented in Fig. 6 for both imperfection shapes. An interesting trend to note is that for small amplitude imperfections, the prebuckling solution (PATH #4) is slightly stabilizing with respect to the classical solution (PATH #3), but as the amplitude ratio increases, the influence of prebuckling response becomes destabilizing. Also, the mode number of the instability increases with increasing amplitude of the imperfection.

The influence of relatively long wavelength (r = 3 and 4)

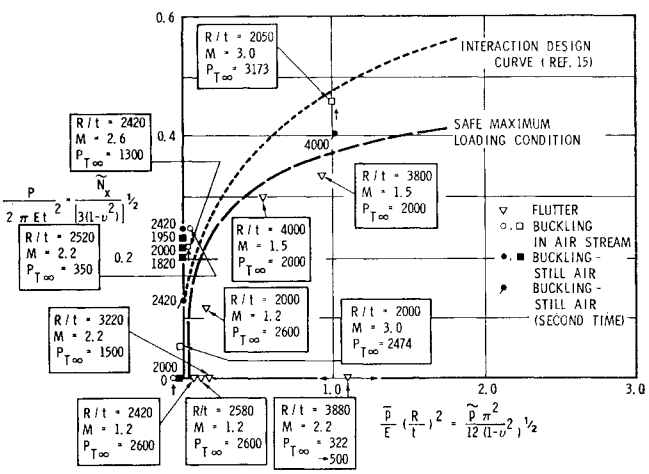

Fig. 8 Buckling interaction curves and loading conditions on aeroelastically unstable shells.

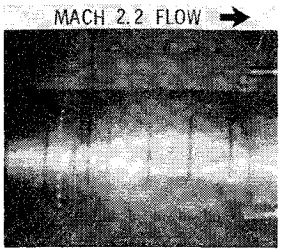

Fig. 9 Elliptical buckled pattern due to radial pressure loading in the presence of a Mach 2.2 air stream.

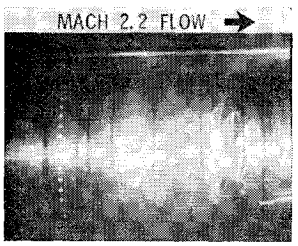

Fig. 10 Diamond buckled pattern due to axial compressive loading in the presence of a Mach 2.2 air stream.

axisymmetric initial imperfections on the aeroelastic stability characteristics of thin cylindrical shells has been investigated previously by the authors.[4] It was observed that the combined influence of initial imperfections and nonlinear prebuckling deformations produced a pronounced destabilizing influence on the flutter boundary obtained with the classical approach. This inclusion of initial geometric imperfections in the stability analysis is seen to represent an over-all improvement in the correlation between theory and experimental observations for cylindrical shell flutter.

3. Experimental Observations

A limited number of experimental observations have been made on the interaction characteristics of the buckling and panel flutter of thin cylindrical shells in the presence of a supersonic flowfield. These observations were obtained on two different wind-tunnel models, an ogive-cylinder model[5,11] and a ducted model.[1,2,12] The most recent experiments were performed on the ogive-cylinder model illustrated in Fig. 7, whereas some of the earlier studies were performed on the ducted model illustrated in Ref. 2. The thin test shells under investigation were located on the cylindrical section near the base of each model. The shell geometries for both models were identical but the local flow conditions, i.e., the boundary-layer characteristics, were different. A brief summary of these studies is presented below along with some recent observations obtained with the ogive model but not reported in the literature.

3.1 Buckling Interaction Curve

All of the experimental buckling studies were concerned with the buckling of circular cylindrical shells under a combined internal pressure and axial compressive end loading, a radial pressure loading only, or an axial compressive loading only. These studies were conducted both with and without the presence of a supersonic flow external to the shell and parallel to its axis.

Initial studies were conducted in still air to determine experimentally a buckling interaction curve for the cylindrical shells of interest. The influence of the airstream was then estimated by comparing shell buckling data taken in the wind tunnel with this experimentally determined still air interaction curve.

Buckling data taken from several tests have been superimposed on the buckling interaction curve illustrated in Fig. 8. The shaded symbols represent points determined from still air buckling studies, whereas the open symbols denote wind-tunnel test points. The flow conditions and radius to thickness ratios are indicated beside each of the test points. The open triangular symbols represent dynamic instabilities observed in Ref. 11 and current wind-tunnel studies. The other open symbols represent static (buckling) instability in the presence of an airstream. A tabulation of these data and their source is presented in Table 1.

Figures 9 and 10 illustrate typical buckle mode patterns observed on two shells buckled in the presence of an airstream. These photographs were taken for the data points indicated by the vertical arrows at the lower internal pressures on the buckling interaction curve. At the data point indicated by the vertical arrow at the higher internal pressure on the buckling interaction curve, an axially symmetric bellows type buckling mode was observed. These buckle mode patterns are qualitatively similar to those obtained in still air buckling studies.[9] The airstream in these cases caused no significant change in the buckling mode patterns. A review of the buckling interaction curve shown in Fig. 8 also indicates that no significant shift occurs in the wind-tunnel buckling points (open nontriangular symbols) when compared to their still air buckling counterparts (dark symbols). On the basis of these limited experimental observations, the supersonic airstream appears to have only a minor influence on the buckling characteristics of cylindrical shells.

3.2 Repeated Buckling of a Cylindrical Shell

Experimental buckling data for a given shell configuration which includes external flow effects is difficult and time consuming to obtain since each shell is permanently damaged after its initial buckling. Each point must be obtained with a new test model and a new wind-tunnel run. In view of this, an alternate procedure described below is being followed to evaluate further the influence of a flowfield on the buckling instability of thin cylindrical shells.

Table 1 Buckling interaction and flutter data

Event	Source	M_∞	P_{T_∞} psf	No. times buckled	P lb	p psi	h in.	R/h	$\bar{N}_x/[3(1-\nu^2)]^{1/2}$	$\bar{p}\pi^2/12(1-\nu^2)^{1/2}$
Buckle	[2]	3.0	2474	1	90	−0.037	0.0040	2000	0.056	−0.009
Buckle	[2]	3.0	3173	1	700	3.93	0.0039	2050	0.458	1.03
Buckle	[2]	0	...	1	390	0	0.0041	1950	0.230	0
Buckle	[2]	0	...	1	350	0	0.0040	2000	0.218	0
Buckle	[2]	0	...	1	400	0	0.0044	1820	0.205	0
Buckle	[2]	0	...	1	0	−0.050	0.0040	2000	0	−0.012
Buckle	Jan. '68	2.6	1300	1	200	0.111	0.0033	2420	0.250	0.047
Buckle	Jan. '69	2.2	350	1	200	0.055	0.0032	2500	0.222	0.025
Buckle	Jan. '66	0	...	2	130	0.900	0.0020	4000	0.406	1.03
Flutter	[11]	1.2	2600	0	0	0.240	0.0033	2420	0	0.100
Flutter	[11]	1.2	2600	0	0	0.270	0.0031	2580	0	0.128
Flutter	[11]	1.5	2000	0	130	0.910	0.0021	3800	0.334	0.940
Flutter	[11]	1.5	2000	0	105	0.480	0.0020	4000	0.298	0.548
Flutter	[11]	1.2	2600	0	210	0.520	0.0040	2000	0.169	0.148

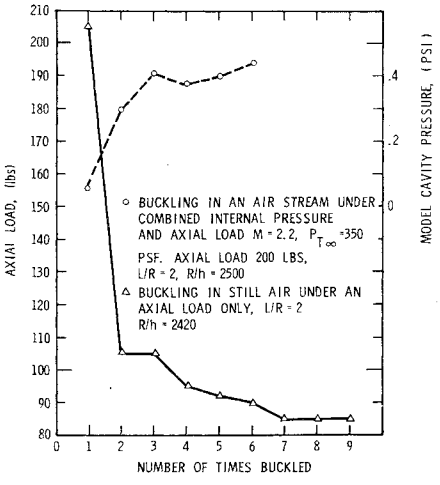

Fig. 11 Shells buckled a repeated number of times to establish an asymptotic buckling load.

In Ref. 13 an experimental study is described that was conducted to determine the buckling load history as a cylindrical shell was repeatedly buckled under axial end loads. It was demonstrated in this study that the buckling load decreases quite rapidly after the first buckling, but finally approached an asymptotic value after the shell was buckled several times. This asymptotic behavior of the buckling load was attributed to the formation of a plastic hinge pattern over the shell. After the shell had been buckled a sufficient number of times, this plastic hinge pattern was fairly well established and the load carrying capacity of the shell determined.

The present authors made similar observations on the cylindrical shell flutter models employed in this study. The results of the observations are shown in Fig. 11, which illustrated the buckling load history of a typical flutter shell that has been repeatedly collapsed under an axial compressive load in still air. Each time after the shell was buckled it was pressurized to eliminate the buckles. The pressure was then removed and the shell was buckled again. After the shell had been buckled several times, subsequent loading revealed that a small local buckle might frequently appear at lower loading levels than that which would cause the shell to suddenly collapse. The loading resulting in a sudden collapse of the shell was always taken as the critical buckling load and not the lower load that initiated a localized small dimple in the shell.

The previous asymptotic behavior of a cylindrical shell also was verified in the wind tunnel for a shell loaded under a combined internal pressure, axial load, and aerodynamic pressure due to the external flowfield. The following experimental procedure was employed. The wind-tunnel flow conditions and axial load were fixed with a high-internal pressure level in the shell. After the test conditions were established, the internal pressure was then reduced until buckling occurred. The shell internal pressure was then increased until the buckles were removed, and the process repeated. A review of the data, illustrated in Fig. 11, indicates that a similar asymptotic character exists for a shell loaded under combined internal pressure and axial load buckling in the presence of an airstream.

Current studies are under investigation to determine the influence of the airstream on this asymptotic buckling load of the shell since it may be a more practical way of evaluating the influence of the airstream on the elastic stability of the shell.

3.3 Interaction of Buckling and Flutter

A few qualitative observations have been made on the interaction of shell buckling and panel flutter during recent wind-tunnel tests. These observations were made both during the actual testing and after studying high-speed films taken during the buckling and/or fluttering occurrence. These observations are presented below.

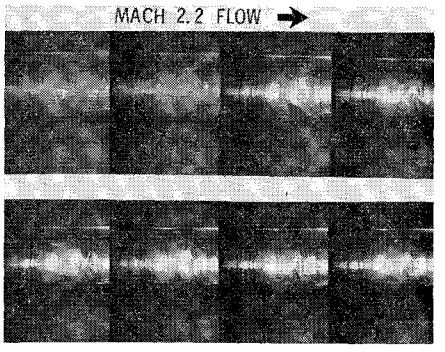

Fig. 12 Shell flutter—diamond buckling transition at $M = 2.2$. Frame speed 400 fps. Flow is from left to right.

For specified flow conditions below a certain critical dynamic pressure, the cylindrical shell was found to be only statically unstable, buckling at a load and into a modal configuration that was not significantly different from that expected for the shell in the absence of an airstream. The specific form of the final modal configuration depended upon the location of the buckle point on the buckling interaction curve as illustrated by Figs. 8–10. Above a critical dynamic pressure level a panel flutter instability occurred at internal stress levels slightly below those levels that would induce shell buckling or divergence. These dynamic instabilities are indicated by the open triangular points on the buckling interaction curve. One observation was made in which the stress level, due to a combined internal pressure and axial load, was increased further to the critical buckling level after flutter was well established on the shell. In this case, the panel flutter instability was completely stabilized by the formation of the diamond pattern buckling mode shape. This is illustrated in the sequence of frames shown in Fig. 12.

In the case of a radial pressure loading only at sufficiently small dynamic pressures, the shell would buckle into the typical buckle mode pattern illustrated in Fig. 9. At dynamic pressures above some critical value a panel flutter instability would occur at stress levels slightly below those that would lead to shell buckling under radial pressure. After panel flutter had been established on the shell and the stress level was changed to induce radial buckling, two different observations were noted. For the relatively thicker shells, (R/h = 2000 to 2500), the shell would buckle into a modal pattern similar to that illustrated in Fig. 9, which appeared to stabilize the shell against flutter.[1] For the thinner shells (R/h = 4000), high-speed movies taken during recent wind-tunnel tests indicated that a postbuckling flutter response would occur. In the latter case, a dynamic instability was observed which was superimposed upon a basic buckling mode similar to that illustrated in Fig. 9. The resulting flutter mode had an apparent wave motion in the circumferential direction of the shell normal to the airstream direction and the major axis of the elliptic shaped buckles. This motion, however, was not as periodic as that found prior to buckling. A circumferentially traveling wave flutter mode shape also has been observed in an earlier test and reported by Olson in Ref. 2.

4. Conclusions

Both theoretical and experimental observations indicate that for the parametric range under consideration, the critical buckling load and circumferential wave number of the static instability of thin cylindrical shells are not significantly influenced by a supersonic flowfield. The theoretical analysis

indicates that the freestream static pressure required to initiate shell flutter is drastically reduced by the addition of only a small amount of axial load. As the character of the instability changes from flutter to static divergence, the critical circumferential wave number changes from a low n number ($n \cong 10$) to an n number corresponding to the still air buckled shape for the shell geometry and internal pressure considered. This trend also was observed experimentally.

The influence of increasing the amplitude of the initial geometric imperfections was found to be destabilizing in both the static buckling and aeroelastic stability studies. The classical buckling analysis predicts a change in the circumferential wave number of the instability from a high n number at zero internal pressure to the axisymmetric instability as the internal pressure is increased. This trend also has been observed experimentally for very thin-walled cylindrical shells.

References

[1] Stearman, R. O., Lock, M. H., and Fung, Y. C., "Ames Tests on the Flutter of Cylindrical Shells," Guggenheim Aeronautical Lab., California Institute of Technology, Structural Dynamics Report SM 62–37, Dec. 1962, California Institute of Technology.

[2] Olson, M. D., "Supersonic Flutter of Circular Cylindrical Shells Subjected to Internal Pressure and Axial Compressions," Guggenheim Aeronautical Lab., California Institute of Technology, Structural Dynamics Report SM 65–7, AFOSR 65-0599, April 1965; California Institute of Technology; see also "Supersonic Flutter of Cylindrical Shells," Ph.D. thesis, 1966, California Institute of Technology; see also *AIAA Journal*, Vol. 5, No. 10, Oct. 1967, pp. 1849–1856; and *AIAA Journal*, Vol. 4, No. 5, May 1966, pp. 858–864.

[3] Carter, L. L. and Stearman, R. O., "Some Aspects of Cylindrical Shell Panel Flutter," *AIAA Journal*, Vol. 6, No. 1, Jan. 1968, pp. 37–43.

[4] Barr, G. W. and Stearman, R. O., "Aeroelastic Stability Characteristics of Cylindrical Shells Considering Imperfections and Edge Constraint," *AIAA Journal*, Vol. 7, No. 5, May 1969, pp. 912–919.

[5] Stearman, R. O., "An Experimental Study on the Aeroelastic Stability of Thin Cylindrical Shells," *Abstracts of the 12th International Congress of Applied Mechanics*, Stanford Univ., Calif., Aug., 1968.

[6] Monta, W. J., Czarnecki, K. R., and Devdikis, W. D., "Drag Due to Two Dimensional Surface Roughness in a Turbulent Boundary Layer at Mach = 3.0 With and Without Heat Transfer," TND-4746, Sept. 1968, NASA.

[7] Franklin, J. N., "On the Numerical Solution of Characteristic Equations in Flutter Analysis," *Journal of the Association of Computing Machinery*, Vol. 5, 1958, pp. 45–51.

[8] Guderley, K. D., "On Nonlinear Eigenvalue Problems for Matrices," *Journal of the Society of Industrial and Applied Mathematics*, Vol. 6, No. 4, Dec. 1958.

[9] Fung, Y. C. and Sechler, E. E., "Instability of Thin Elastic Shells," *Structural Mechanics, Proceedings of First Symposium on Naval Structural Mechanics*, Pergamon Press, New York, 1960.

[10] Almroth, B. O., "Influence of Edge Conditions on the Stability of Axially Compressed Cylindrical Shells," CR-161, Feb. 1965, NASA.

[11] Stearman, R. O., "An Experimental Study on the Aeroelastic Stability of Thin Cylindrical Shells of the Lower Supersonic Mach Numbers," Final Technical Rept. 66–2828, Air Force Office of Scientific Research, and ARL 67–0006, Dec. 1966, Aeronautical Research Lab.

[12] Fung, Y. C., "Interaction of Mechanical and Aeroelastic Instabilities of a Circular Cylindrical Shell," *Dynamic Stability of Structures*, Pergamon Press, New York, 1966.

[13] Horton, W. H. and Durham, S. C., "Repeated Buckling of Circular Cylindrical Shells and Conical Frusta by Axial Compressive Forces," SUDAER Rept. 175, AD439013, Nov. 1963, Stanford Univ.

[14] Almroth, B. O., "Influence of Imperfections and Edge Restraint on the Buckling of Axially Compressed Cylinders," CR-432, April 1966, NASA.

[15] Weingarten, V. I., Morgan, E. J., and Seide, P., "Final Report on Development of Design Criteria for Elastic Stability of Thin Shell Structures," STL/TR-60–0000–19425, Dec. 31, 1960, Space Technology Labs Inc.